Ternary and quaternary Lennard-Jones atomic clusters: the effects of atomic sizes on the compositions, geometries, and relative stability

Hiroshi Takeuchi*

Division of Chemistry, Graduate School of Science, Hokkaido University, Sapporo 060-0810, Japan

Corresponding author phone: +81-11-706-3533; Fax: +81-11-706-3501; e-mail: takehi@sci.hokudai.ac.jp

Abstract: Global-minimum geometries of ternary and quaternary Lennard-Jones clusters have been calculated with constraints on atomic compositions of the clusters. In the present study, the constraints were removed to obtain optimal compositions. The size ratios of the largest-sized atom to the smallest-sized one ranged from 1.1 to 1.6 whereas the depths of the interatomic potentials were constant. The heuristic method combined with the geometrical perturbations and atom-type conversion was used to search for the global minima of the clusters with up to 50 atoms. The smallest-sized and largest-sized atoms usually occupy cores and outer shells, respectively, and the atoms with intermediate sizes are often lacking. The size ratio has pronounced effects on the compositions, structures, and relative stability of the clusters.

Keywords: Global optimization; Atom-type conversion; Core-shell structures.

1. Introduction

Nanoclusters have peculiar properties compared with bulk matters since the cluster is much smaller than the bulk material in size. Chemical and physical properties of nanoclusters significantly depend on the structures. They have been experimentally studied with spectroscopic and diffraction techniques and theoretically investigated employing global optimization methods and simulations. At present, homoclusters with a few hundred atoms are tractable using theoretical approaches. Compared with homoclusters, heteroclusters show considerably complicated structural behavior because a lot of combinations of constituent particles of different types are possible. The complication is an important feature of the heteroclusters since it may induce new structures and thus new properties. Many investigations on metallic heteroclusters have been reported as described in the review by Ferrando et al. [1] because of great interest in catalysis, and optical and magnetic properties of the clusters.

As mentioned before, the atomic composition of a heterocluster [2–12] makes the structure prediction complicated. Hence geometry optimizations of multicomponent clusters are still challenging. For one of the simplest multicomponent clusters, binary Lennard-Jones (BLJ) clusters, the putative global minima of the clusters with up to 100 atoms are reported in the literature [2–8]. The potential energy of the N-atom BLJ cluster (BLJ_N) is calculated using the interatomic potential $V(i, j)$:

$$E_N = \sum_{i<j}^{N} V(i,j) = 4\sum_{i<j}^{N} \varepsilon_{\alpha\beta}\left[\left(\frac{\sigma_{\alpha\beta}}{r_{ij}}\right)^{12} - \left(\frac{\sigma_{\alpha\beta}}{r_{ij}}\right)^{6}\right] \quad (1)$$

Here r_{ij} represents the distance between atoms i and j, and α and β mean the types of the atoms i and j (represented by A and B), respectively. The evaluation of eq (1) is performed with the relation of $\varepsilon_{AA} = \varepsilon_{BB} = \varepsilon_{AB} = \varepsilon$ in the literature [2–8]. The size parameters, σ_{AA} and σ_{BB}, are set to be $S_A\sigma$ and $S_B\sigma$, respectively, and the σ_{AB} value is equal to $(\sigma_{AA} + \sigma_{BB})/2$ according to the Lorentz rule. The value of S_A is 1 and the parameter S_B (= σ_{BB}/σ_{AA}) is a predefined constant representing the size ratio of the B atom to the A atom.

The original investigation on the BLJ clusters was performed by Doye and Meyer [2]. The study was aimed at elucidating the effect of the size of the B atom (S_B = 1.05, 1.1, 1.15, 1.2, 1.25, 1.3) on the

global minima of the BLJ clusters with 5 to 100 atoms. Subsequently to this, Cassioli et al. [3], Marques and Pereira [4], Kolossváry and Bowers [5], Sicher et al., [6], Tao et al. [7], and Rondina and Da Silva [8] proposed different optimization algorithms to search for global minima of the BLJ clusters. The lowest-energy geometries obtained in the previous studies are tabulated in the Cambridge Cluster Database [13]. Takeuchi [14] also optimized the geometries of BLJ_5 to BLJ_{100} with $S_B = 1.05 – 1.3$, and those of BLJ_5 to BLJ_{50} with $S_B = 1.4 – 2.0$. It was found that the existence of fairly large-sized atoms ($S_B \geq 1.6$) induces complicated structural growth sequence.

For ternary LJ clusters $A_lB_mC_n$ ($N = l + m + n$), Wu and coworkers [9, 10] examined the effect of the size parameters, σ_{BB} and σ_{CC} ($= S_C\sigma$), on the global-minimum geometries. In these studies, the clusters are defined as follows: (i) $l = m = n = 10$, $1.0 \leq S_B \leq 1.3$, $1.0 \leq S_C \leq 1.3$ [9]; (ii) $N = 9 – 55$ ($l : m : n \cong 1 : 1: 1$), (S_B , S_C) = (1.1, 1.2), (1.2, 1.4) [9]; (iii) $l = 13$, $m + n = 42$, $S_B = 1.05$, $S_C = 1.1$ [9]; (iv) $l = 12$, $m = n = 13$, $1.0 \leq S_B \leq 1.4$, $1.0 \leq S_C \leq 1.4$ [10]. They also calculated the global-minimum structures of noble gas systems of $Ar_{12}Kr_mXe_n$ ($m + n = 26$) [10], $Ar_{13}Kr_mXe_n$ ($m + n = 42$) [10], $Ar_{19}Kr_mXe_{19}$ ($m = 0 – 17$) [11], $Ar_{19}Kr_{19}Xe_m$ ($m = 0 – 17$) [11], and $Ar_mKr_{19}Xe_{19}$ ($m = 0 – 17$) [11]. Dieterich and Hartke [12] investigated cluster systems of binary to quinary mixtures ($He_{19}Xe_{19}$, $Ar_{19}Kr_{19}$, $Ar_{32}Kr_6$, $Ar_{13}Kr_{13}Xe_{12}$, $Ar_{18}Kr_{19}Xe$, $He_2Ne_2Ar_5Kr_5Xe_5$, $He_{11}Ne_{11}Ar_{11}Kr_{11}Xe_{11}$) to demonstrate the effects of compositional changes on the structures. In the above studies [9 – 12], the atomic compositions are partially or completely fixed and the cluster sizes are rather limited in some cases. Hence global minima of the LJ clusters with at least three components have never been elucidated. Important issues on the ternary LJ (TLJ) and quaternary LJ (QLJ) clusters, structural growth sequence (size-dependent evolution of the structures) and relative stability, are still unsettled.

For bimetallic clusters, a lot of investigations have reported the effects of the compositions on the structures [1]. Factors such as surface energies, cohensive energies, relative atomic sizes, and bond strengths are taken into account to understand properties of the clusters. Recent studies [15 – 27] on

bimetallic and trimetallic clusters examine the structures as the function of the cluster size and atomic composition. The other systems of binary clusters are also investigated in [28 – 33].

As well known in the studies on the LJ homoclusters [34 – 41], the number of stable configurations of the cluster drastically increases with increasing cluster size. The minima corresponding to the stable configurations are separated by barriers and the barrier heights prevent optimization methods from searching for global minima. In addition to this difficulty, heteroclusters exhibits a lot of atomic compositions. The optimization of the composition has been treated with the following two strategies. One is to convert the type of an atom in the optimization algorithm. The other is to exchange two atoms of different types. In this approach, the atomic composition of the cluster is invariant and thus calculations are repeated for different compositions. The former approach directly optimizes the composition of the system. In Refs [2 – 5, 7, 14], the atom-type conversion was used in the optimization of the BLJ clusters. The case study in the literature [7] suggests that the atom-type conversion is efficient for searching for the global minima of the clusters expressed by pair potentials with the constant well depth since the conversion significantly reduces the potential energy.

The present study was undertaken to examine the structures of the TLJ and QLJ clusters with emphasis on the effects of the atomic sizes on the compositions, structures, and relative stability of the clusters. The heuristic method combined with geometrical perturbations and atom-type conversion (HMGPAC) [14] was used to optimize the structures of these clusters. Since the efficiency of the atom-type conversion was not discussed in detail [2 – 5, 7, 14], its performance was examined using the calculated results.

2. Optimization method

The geometry optimization starts from configurations randomly generated. For the TLJ clusters, the numbers of the atoms of three types N_α (α = A, B, and C) are randomly selected. The atoms are placed within a sphere with the volume of $\sum_\alpha N_\alpha \left(r_{\mathrm{e},\alpha}\right)^3$ where $r_{\mathrm{e},\alpha} = \sqrt[6]{2}\sigma_{\alpha\alpha}$. The geometry is

locally optimized with a limited memory quasi-Newton method (L-BFGS [42]). Then the type of an atom is twice converted: the type A is changed in the order, B, C; the type B is changed in the order, C, A; and the type C is changed in the order, A, B. After a conversion, the geometry is optimized by the L-BFGS [42] method. If the potential energy of the cluster is improved with the conversion followed by local optimization, the cluster geometry and atom type are updated. Finally the atom-type conversion is $2N$ times performed for all the atoms.

After the atom-type conversion is finished, the geometry is optimized with two geometrical perturbation operators (surface and interior operators). These operators move an atom or some atoms with the highest potential energy to positions which are expected to decrease the potential energy of the cluster. The positions are selected from the neighborhood of either the cluster center or the surface. The local optimization due to the L-BFGS [42] method is performed for the geometries created with the operators to locate new local minima. The two operators are briefly described below (the detail of them is given in [14, 40]).

The interior operator moves the selected atoms to the surface of the sphere which takes the radius of $r_{e,\alpha}/2$ and the center coincident with the center of mass of the cluster. The number of the moved atoms [14] is randomly selected from 1 to 5. If the potential energy of the cluster is not improved during the last ten interior operators followed by local optimizations, the surface operator is carried out. Stable positions on the surface of the cluster are examined and the best positions are chosen from them as the positions of the moved atoms. If the energy of the cluster is not improved by moving the highest-energy atom, the second highest-energy atom and the third highest-energy atom are separately moved [14]. The number of the moved atoms is initially 1 and increases up to 4 at an interval of 1 if the energy of the cluster is not improved. When energy-lowering is observed, the number is initialized and the cluster geometry is updated. When the surface operator with 4 moved atoms does not improve the energy of the cluster, the optimization algorithm returns to the atom-type conversion. In a run, a series of the atom-type conversion, the interior operator, and the surface operator is repeated. The

termination condition of the run is that the lowest energy obtained before the atom-type conversion is invariant compared with that obtained after the surface operator.

The QLJ clusters take atoms of an additional type D ($\sigma_{DD} = S_D\sigma$). The initial compositions of the clusters are randomly determined. With the atom-conversion operator, the type A is changed in the order, B, C, D. Similarly the type B is changed in the order, C, D, A, the type C is changed in the order, D, A, B, and the type D is changed in the order, A, B, C. Consequently, the atom-type conversion is $3N$ times carried out.

For the TLJ clusters, 6 sets of (S_A, S_B, S_C) were used: (1.0, 1.05, 1.1), (1.0, 1.1, 1.2), (1.0, 1.15, 1.3), (1.0, 1.2, 1.4), (1.0, 1.25, 1.5), and (1.0, 1.3, 1.6). The sets of (S_A, S_B, S_C, S_D) for the QLJ clusters were (1.0, 1.05, 1.1, 1.15), (1.0, 1.1, 1.2, 1.3), (1.0, 1.15, 1.3, 1.45), and (1.0, 1.2, 1.4, 1.6). Since the size parameters grow in an arithmetical progression, the parameters S_C and S_D are used to define the TLJ and QLJ clusters, respectively.

Since the present method adopts a monotonic descent algorithm, the energy of the final geometry is lowest in the run. The computations were performed on dual core 3 GHz Intel Xeon 5160 processors. No parallel computation was carried out. With HMGPAC, a run for the 50-atom TLJ cluster was completed in 5 s and the corresponding time needed for the 50-atom QLJ cluster was 7 s.

3. Results

The putative global minimum of each cluster could be located many times from 1000 initial geometries. In a few cases, however, 15000 initial geometries were necessary to locate the global minimum twice or third times. The potential energies and geometries of the putative global minima of the clusters are tabulated in supplementary data together with the number of the initial geometries and the number of the runs in which the final geometries correspond to the putative global minima. In the present method, the local optimization is always carried out for each of the geometries generated initially and with the atom-type conversion, interior and surface operators. Hence the average number

of the local optimizations performed in one run is also listed in the supplementary data as an indicator of the performance of the method.

3.1. Structural features

The optimal atomic compositions of the TLJ clusters are shown in Figure 1. The results show that the compositions of the TLJ clusters depend on the sizes of the constituent atoms. The A atoms coexist with the C atoms whereas the B atom is lacking in a lot of the clusters. In the series of the clusters with S_C = 1.4, the number of the C atoms is strikingly large for N = 36 – 40. The similar trend is found for the TLJ(S_C = 1.5) clusters with N = 35 – 38. The structural motifs of these clusters are different from those of the other clusters as described later.

To investigate the distribution of the atoms in the TLJ cluster, the distances between the center of mass and the atoms were averaged for each of the atom types as follows:

$$R_{\mathrm{ave}} = \frac{1}{N_\alpha}\sum_{k=1}^{N_\alpha}|\overrightarrow{r_k} - \overrightarrow{r_{\mathrm{cm}}}|, \qquad \alpha = \mathrm{A, B, or C} \tag{2}$$

Here $\overrightarrow{r_{\mathrm{k}}}$ and $\overrightarrow{r_{\mathrm{cm}}}$ represent the vectors directed to the position of the atom of the type α and to the center of mass, respectively. The obtained results are shown in Figure 2. For the TLJ(S_C = 1.1) clusters with N = 48 – 50, the values of R_{ave} for the B atom are close to zero. For each of the other clusters, the A and C atoms usually take the smallest and largest R_{ave} values, respectively. Accordingly, the A atoms occupy cores of the clusters whereas the C atoms construct outer shells. The R_{ave} values for the B atoms are usually larger than those for the A atoms, indicating that the B atoms exist on the A atom core.

The compositions of the QLJ clusters are shown in Figure 3 together with the average distances. The intermediate-sized atoms (B and C) are often lacking in the clusters. In the QLJ clusters as well as the TLJ clusters, the smallest-sized atoms form cores and the larger-sized atoms occupy outer surfaces. The number of the D atoms is significantly large in the QLJ(S_D = 1.45) clusters with N = 35 – 40 as found in some of the TLJ(S_C = 1.4, 1.5) clusters. The numbers of the A and D atoms in the QLJ

clusters with S_D = 1.15, 1.3, 1.45, 1.6 are similar to those of the A and C atoms in the TLJ clusters with S_C = 1.1, 1.3, 1.4, 1.6, respectively.

The number of atoms surrounding a core atom (coordination number for an A atom) was analyzed to extract features of the global-minimum structures. In the analysis, the coordinated atom satisfies the following condition: the distance between the coordinated and core atoms is shorter than a tentative cutoff distance (1.2 times as long as the equilibrium interatomic distance). The clusters with less than 12 coordination atoms are marked with plus in Figure 4. The other clusters take the maximum coordination number of 12. Geometries formed by 12 coordination atoms were classified into the icosahedron, elongated pentagonal dipyramid (Ino decahedron), and triangular orthobicupola. These polyhedra are also found in the BLJ clusters with $S_B \leq 1.6$ [14]. The clusters marked with closed circles in Figure 4 include at least one icosahedron and the maximum number of the icosahedra is 15. Each of the clusters marked with open circles has a triangular orthobicupola as the local structure and contains no intermediate-sized atoms. In the cluster marked with the open square, 1, 2, or 3 elongated pentagonal dipyramids coexist with at least one icosahedron. The structural growth sequence pattern of the TLJ clusters is similar to that of the QLJ clusters when the value of S_C(TLJ) is equal or close to that of S_D(QLJ). Hence the largest atom sizes are correlated with the structural growth sequence patterns of the clusters as well as the atomic compositions.

3.2. Relative stability

The relative stability of the cluster is calculated using the equation

$$S_N = E_{N+1} + E_{N-1} - 2E_N \qquad (3)$$

The results obtained for the TLJ and QLJ clusters are shown in Figure 5; a positive value of S_N means that the N-atom cluster is stable compared with the ($N \pm 1$)-atom clusters. As shown in the figure, most of the clusters with N = 13, 19, 23, 26, 29, 32, 34, 37, 39, 41, 45, 48 (marked with dashed lines) are relatively stable. A few exceptions are observed for the TLJ(S_C = 1.6) clusters with N = 31, 33, 47 and the QLJ(S_D = 1.6) clusters with N = 31, 33. The QLJ(S_D = 1.6) clusters with N = 31, 33 are identical to the TLJ(S_C = 1.6) clusters with N = 31, 33 since these clusters have no intermediate-sized

atoms. It is important to note that the positions of the positive peaks for the TLJ clusters with S_C = 1.1, 1.3, 1.4, 1.6 are similar to those for the QLJ clusters with S_D = 1.15, 1.3, 1.45, 1.6, respectively. This is consistent with the results on the atomic compositions and structural growth sequence patterns.

3.3. Efficiency of the optimization method

The number of local optimizations N_{opt} required for searching for the global minimum once is a useful parameter to evaluate the efficiency of the optimization algorithm. It was calculated from the data in Tables S1 and S2 (the number of the initial geometries, the number of the runs in which the final geometries correspond to the putative global minima, and the average number of the local optimizations performed in one run). The results obtained for the TLJ and QLJ clusters are shown in Figures 6 and 7, respectively. The large N_{opt} values indicate that it is difficult to obtain the global minima of the clusters. In Figure 6, the data of the TLJ clusters are compared with those of the BLJ clusters; the values of N_{opt} of the TLJ clusters are usually larger than the corresponding ones of the BLJ clusters. The N_{opt} values for the TLJ clusters tend to increase with increasing S_C and the similar trend is found for the QLJ clusters. Hence, the inclusion of large-sized atoms in the multicomponent clusters lowers the ability of HMGPAC to search for the global minima.

The efficiency of HMGPAC is determined by the ability of the interior, surface, and atom-type conversion operators to lower potential energies. Figure 8 shows the energy lowering due to each operator for the series of the TLJ(S_C = 1.6) clusters; the numerical data were obtained from the results of the runs in which the global minima were located. The atom-type conversion considerably reduces the energies of the clusters. This is found for the clusters under investigation.

4. Discussion

4.1 Compositions, structures, and relative stability

In the TLJ and QLJ clusters, the large-sized atoms prefer occupying the outer shell as shown in Figures 2 and 3. This is also found for the BLJ clusters [14]. The cohesive energy of the atoms is independent of the atom types because the potential parameter $\varepsilon_{\alpha\beta}$ in eq (1) is constant. On the other

hand, the surface energy of the large-sized atoms is smaller than that of the small-sized atoms. As described in [1], the particles with lower surface energy tend to segregate to the surface and smaller-sized particles tend to occupy the core. This is consistent with the global-minimum geometries of the TLJ and QLJ clusters. The clusters under investigation would prefer the situation that the number of surface particles is small since they are less stable than core particles. Accordingly, in the TLJ and QLJ clusters, the large-sized and small-sized atoms occupy the surface and core, respectively.

In a lot of the TLJ(S_C = 1.1) clusters, the number of the B atoms is zero as shown in Figure 1. As shown in Figure 4, most of the TLJ(S_C = 1.1) take polyicosahedral structures. In a regular icosahedron formed by the same-type atoms, the distance between the central and outer atoms are shorter than that between the nearest neighboring outer atoms. The ratio of the former distance to the latter one is 1 : 1.05 and thus the central atom is compressed by the outer atoms. For the TLJ(S_C = 1.1) clusters, the ratio of the equilibrium A...C distance to the corresponding C...C distance (1.05 : 1.1) is close to the above-mentioned ratio 1 : 1.05. To release the strain on the central atom, the TLJ(S_C = 1.1) clusters are considered to mainly consist of the A and C atoms.

In the TLJ(S_C = 1.2) clusters, the A and B atoms takes suitable sizes (S_A = 1.0 and S_B = 1.1) to release the strain in the icosahedron. However, Figure 1 shows that the number of the B atoms is much smaller than that of the C atoms. This indicates that the surface energy of the C atoms significantly contributes to the stability of the TLJ(S_C = 1.2) clusters. This would be the case for the other TLJ clusters.

The increase of the size of the C atom leads to the expansion of the outer surface area. To properly keep close contacts between the core and surface in the TLJ(S_C = 1.2 – 1.6) cluster, the core formed by the A atoms is expanded by increasing the number of the A atoms and/or the surface area is reduced by substitution of the B atom for the C atom. Consequently the compositions of the TLJ clusters depend on the atom sizes.

The icosahedron is stable as indicated by the positive peaks at N = 13 in Figure 5. The relative stability of the clusters with N = 13, 19, 23, 26, 29, 32, 34, 37, 39, 41, 45, 48 can be explained by the

formation of a new icosahedron at these sizes. The other structural segments, the elongated pentagonal dipyramid and triangular orthobicupola, are not considered as stability factors of the TLJ and QLJ clusters since these structures in the isolated state converge to icosahedra by local optimization. These segments are stabilized by atoms surrounding them. Hence the structures formed by the surrounding atoms are important to understand the stability of the clusters including the segments.

The relatively stable clusters (N = 31, 33) have the segment of the triangular orthobicupola (Figure 4) and their stability can be explained in terms of the structure of the surface. The cores of the clusters are covered with many triangles and squares formed by the outer atoms. Since the lengths of the sides of the triangles and squares are close to the equilibrium distances, no atom can be embedded in the surfaces. These close contacts between the surface atoms results in the relative stability of these clusters. The similar factor leads to the stability of the TLJ(S_C = 1.6) cluster with N = 47. This is the case for the icosahedron found in most of the clusters since it has 30 close contacts in the surface.

The atomic compositions, structural growth sequence patterns, and relative stability of the QLJ clusters are similar to those of the corresponding TLJ clusters. Hence the features of the QLJ clusters can be understood by the factors described above for the TLJ clusters, that is, the strain in the icosahedron, close contacts between cores and outer surfaces, surface energies of the largest-sized atoms, and close contacts between surface atoms control the above features of the QLJ clusters.

4.2. Efficiency of the method

As mentioned before, the efficiency of HMGPAC depends on the largest atom size in the cluster. The large difference between atomic sizes enhances geometrical variety, as inferred from the structural features in Figure 4. This might make it more difficult to locate the global minimum.

The atom-type conversion is the important step determining the performance of the present optimization method as shown in Figure 8. Since the clusters are randomly generated, the atomic composition is improved with the atom-type conversion operator. The perturbation induced by the atom-type conversion for an atom would diffuse to its surrounding atoms through the local optimization process. The atom-type conversion for interior atoms is considered to be very efficient since the

energy of the atoms near the center of the mass of the cluster contributes to the total energy of the cluster more significantly than that of the surface atoms. The atom-type conversion must be associated with improvement of the whole geometry of the cluster as well as that of the atomic composition, leading to its high efficiency.

5. Conclusions

The present study is aimed at studying atom-size-induced compositions and structural features of the multicomponent clusters under the condition that the depths of the interatomic potentials are constant. The heuristic method combined with the atom-type conversion, interior, and surface operators was applied to the ternary and quaternary LJ clusters with up to 50 atoms. The atom-type conversion operator was crucial for the geometry optimization of the multicomponent clusters because it significantly lowered the potential energy. Most of the clusters have icosahedral segments with the largest-sized and smallest-sized atoms occupying the surfaces and cores, respectively. The intermediate-sized atoms are often lacking in the clusters. The largest-sized atoms considerably affect the compositions and structural growth sequence patterns of the clusters. This means that the ratio of the largest-sized atom to the smallest-sized atom is an essential factor controlling features of the multicomponent LJ clusters. The stability of the clusters can be explained with the network of the close interatomic contacts.

Appendix A. Supplementary data

Supplementary data associated with this article can be found, in the online version, at http://dx.doi.org/xxxxx.

References

[1] R. Ferrando, J. Jellinek, R.L. Johnston, Chem. Rev. 108 (2008) 845.

[2] J.P.K. Doye, L. Meyer, Phys. Rev. Lett. 95 (2005) 063401.

[3] A. Cassioli, M. Locatelli, F. Schoen, Optim. Methods Software 24 (2009) 819.

[4] J.M.C. Marques, F.B. Pereira, Chem. Phys. Lett. 485 (2010) 211.

[5] I. Kolossváry, K.J. Bowers, Phy. Rev. E 82 (2010) 056711.

[6] M. Sicher, S. Mohr, S. Goedecker, J. Chem. Phys. 134 (2011) 044106.

[7] Y. Tao, X. Ruchu, H. Wenqi, J. Chem. Inf. Model. 51 (2011) 572.

[8] G.G. Rondina, J.L.F. Da Silva, J. Chem. Inf. Model. 53 (2013) 2282.

[9] X. Wu, Y. Sun, C. Li, W. Yang, J. Phys. Chem. A 116 (2012) 8218.

[10] X. Wu, C. Huang, Y. Sun, G. Wu, Chem. Phys. 415 (2013) 69.

[11] X. Wu, Y. Sun, Y. Gao, G. Wu, J. Mol. Model. 19 (2013) 3119.

[12] J.M. Dieterich, B. Hartke, J. Comput. Chem. 32 (2011) 1377.

[13] D. J. Wales, J. P. K. Doye, A. Dullweber, M. P. Hodges, F. Y. Naumkin, F. Calvo, J. Hernández-Rojas, T. F. Middleton, The Cambridge Cluster Database, http://www-wales.ch.cam.ac.uk/CCD.html.

[14] H. Takeuchi, Comput. Theoret. Chem. 1050 (2014) 68.

[15] A. A. Dzhurakhalov, I. Atanasov, M. Hou, Phys. Rev. B 77 (2008) 115415.

[16] F. Pittaway, L. O. Paz-Borbón, R. L. Johnston, H. Arslan, R. Ferrando, C. Mottet, G. Barcaro, A. Fortunelli, J. Phys. Chem. C 113 (2009) 9141.

[17] X. Wu, Y. Dong, New J. Chem. 38 (2014) 4893.

[18] D. Bochicchio, R. Ferrando, R. Novakovic, E. Panizon, G. Rossi, Phys. Chem. Chem. Phys. 16 (2014) 26478.

[19] G. Wu, Q. Liu, X. Wu, Chem. Phys. Lett. 620 (2015) 92.

[20] G. Rossi, R. Ferrando, A. Rapallo, A. Fortunelli, B. C. Curley, L. D. Lloyd, R. L. Johnston, J. Chem. Phys. 122 (2005) 194309.

[21] A. Rapallo, G. Rossi, R. Ferrando, A. Fortunelli, B. C. Curley, L. D. Lloyd, G. M. Tarbuck, R. L. Johnston, J. Chem. Phys. 122 (2005) 194308.

[22] X. Lai, R. Xu, W. Huang, J. Chem. Phys. 135 (2011) 164109.

[23] D. Bochicchio, F. Negro, R. Ferrando, Comput. Theoret. Chem. 1021 (2013) 177.

[24] F. Calvo, E. Cottancin, M. Broyer, Phys. Rev. B 77 (2008) 121406(R).

[25] F. Calvo, C. Mottet, Phys. Rev. B 84 (2011) 035409.

[26] M. Molayem, V. G. Grigoryan, M. Springborg, J. Phys. Chem. C, 115 (2011) 7179.

[27] M. Molayem, V. G. Grigoryan, M. Springborg, J. Phys. Chem. C, 115 (2011) 22148.

[28] J. M. C. Marques, F. B. Pereira, J. Comput. Chem. 34 (2013) 505.

[29] F. Calvo, E. Yurtsever, Phys. Rev. B 70 (2004) 045423.

[30] L. J. Munro, A. Tharrington, K. D. Jordan, Comput. Phys. Commun. 145 (2002) 1.

[31] I.L. Garzon, X.P. Long, R. Kawai, J.H. Weare, Chem. Phys. Lett. 158 (1989) 525.

[32] D. Parodi, R. Ferrando, Phys. Lett. 367 (2007) 215.

[33] F. Calvo, E. Yurtsever, Comput. Theoret. Chem. 1021 (2013) 7.

[34] D. J. Wales, J.P.K. Doye, J. Phys. Chem. A 101 (1997) 5111.

[35] X. Shao, H. Jiang, W. Cai, J. Chem. Inf. Comput. Sci. 44 (2004) 193.

[36] Y. Xiang, H. Jiang, W. Cai, X. Shao, J. Phys. Chem. A 108 (2004) 3586.

[37] C. Barrón, S. Gómez, D. Romero, A. Saavedra, Appl. Math. Lett. 12 (1999) 85.

[38] D. M. Deaven, N. Tit, J. R. Morris, K. M. Ho, Chem. Phys. Lett. 256 (1996) 195.

[39] B. Hartke, J. Comput. Chem. 20 (1999) 1752.

[40] H. Takeuchi, J. Chem. Inf. Model. 46 (2006) 2066.

[41] X. Shao, L. Cheng, W. Cai, J. Comput. Chem. 25 (2004) 1693.

[42] D. C. Liu, J. Nocedal, Math. Prog. 45 (1989) 503.

Figure Captions

Figure 1. The numbers of the A, B, and C atoms (N_A, N_B, and N_C) in the ternary Lennard-Jones clusters with S_C = 1.1, 1.2, 1.3, 1.4, 1.5, 1.6.

Figure 2. Average distances R_{ave} between the center of mass and the atoms calculated for each of the atom types A, B, and C in the ternary Lennard-Jones clusters with S_C = 1.1, 1.2, 1.3, 1.4, 1.5, 1.6.

Figure 3. Atomic compositions and interatomic distances of the quaternary Lennard-Jones clusters with S_D = 1.15, 1.3, 1.45, 1.6: left panels, the numbers of the A, B, C, and D atoms (N_A, N_B, N_C, and N_D); right panels, average distances R_{ave} between the center of mass and the atoms calculated for each of the atom types A, B, C, and D.

Figure 4. Structures of the segments in the ternary and quaternary Lennard-Jones clusters. When the coordination number obtained for the cluster is smaller than 12, it is designated with a plus symbol. To distinguish the geometries formed by 12 coordination atoms, 3 symbols are used: closed circle, icosahedron; open square, mixture of icosahedron and elongated pentagonal dipyramid; open circle; triangular orthobicupola.

Figure 5. Relative stability S_N of the global-minimum geometries of the ternary and quaternary Lennard-Jones clusters. Dashed lines show typical magic numbers. (a) The results of the ternary Lennard-Jones clusters with S_C = 1.1, 1.2, 1.3, 1.4, 1.5, 1.6. The data for S_C = 1.2 to 1.6 are offset vertically by $50(S_C - 1.1)$ for clarity. (b) The results of the quaternary Lennard-Jones clusters with S_D = 1.15, 1.3, 1.45, 1.6. The data for S_D = 1.3 to 1.6 are offset vertically by $100/3 \cdot (S_D - 1.15)$ for clarity.

Figure 6. The number of local optimizations N_{opt} required for searching for the global minimum of the ternary Lennard-Jones cluster together with that of the corresponding binary Lennard-Jones cluster.

Figure 7. The number of local optimizations N_{opt} required for searching for the global minimum of the quaternary Lennard-Jones cluster.

Figure 8. Energy lowering ΔE due to the atom-type conversion, interior, and surface operators which is obtained for the ternary Lennard-Jones clusters with S_C = 1.6. The data for the interior and surface operators are multiplied by 5.

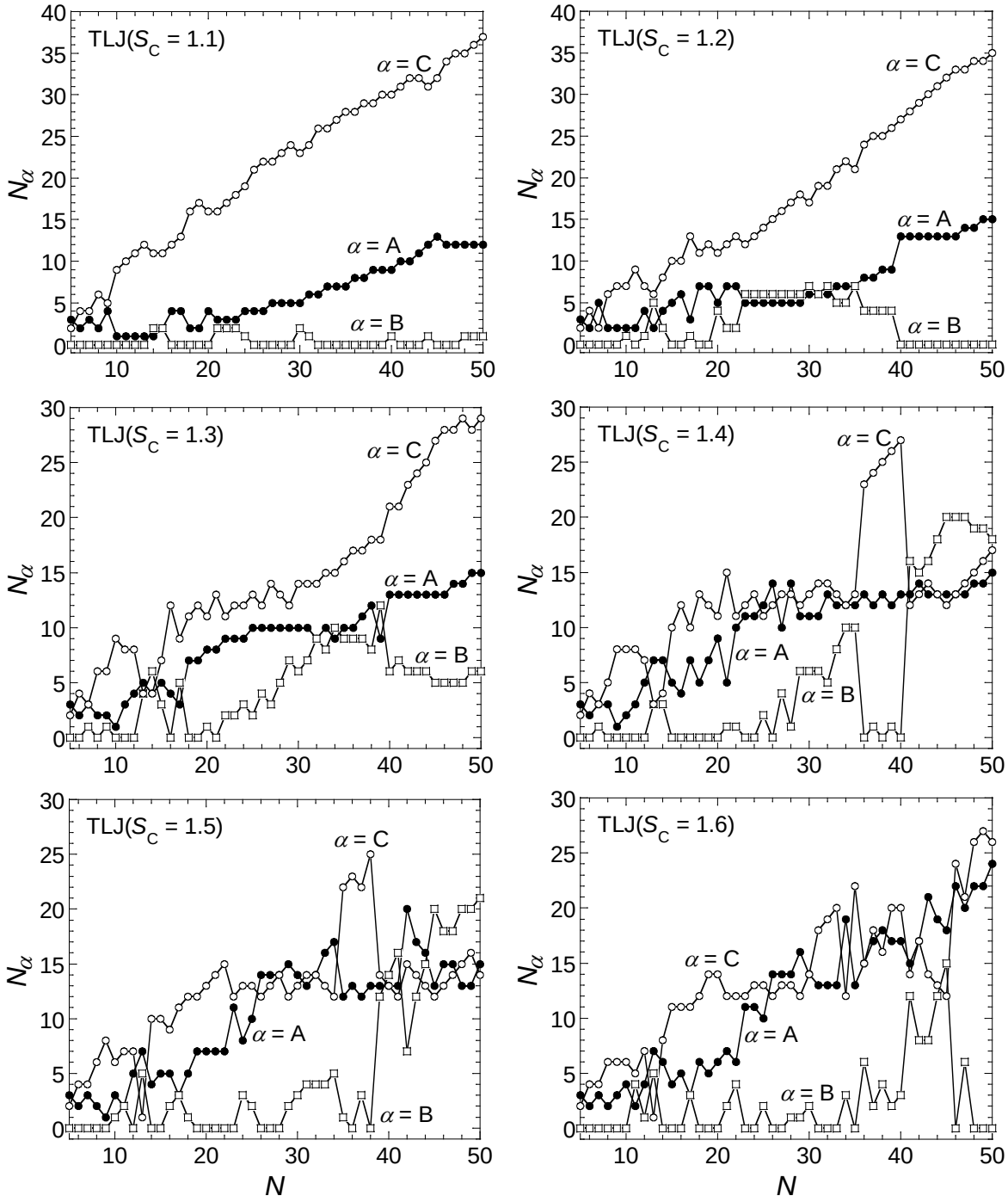
TLJ(S_C = 1.1)
TLJ(S_C = 1.2)
TLJ(S_C = 1.3)
TLJ(S_C = 1.4)
TLJ(S_C = 1.5)
TLJ(S_C = 1.6)
α = C
α = A
α = B
N_α
N

Figure 1

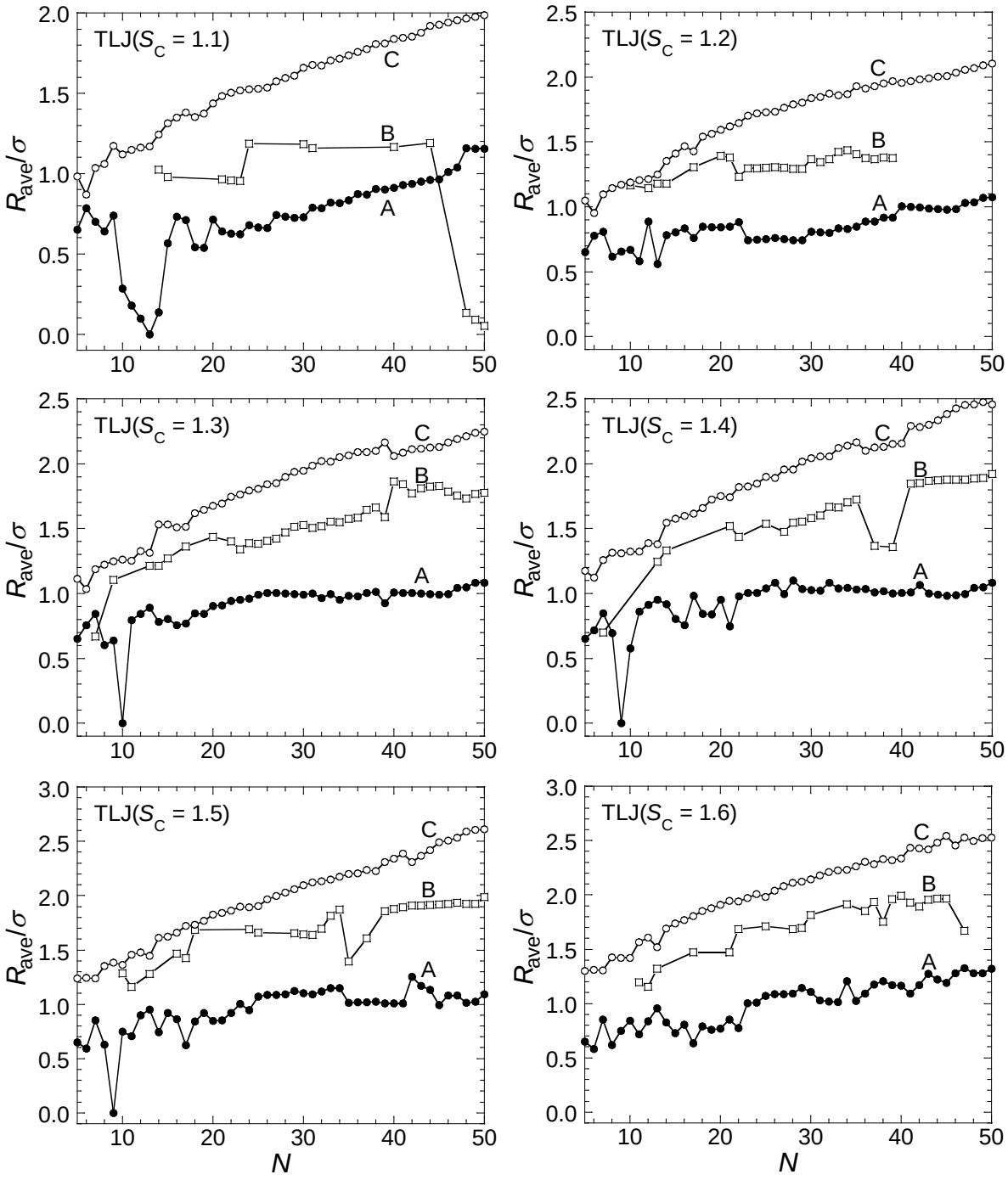
TLJ(S_C = 1.1)
TLJ(S_C = 1.2)
TLJ(S_C = 1.3)
TLJ(S_C = 1.4)
TLJ(S_C = 1.5)
TLJ(S_C = 1.6)
R_{ave}/σ
N
A
B
C

Figure 2

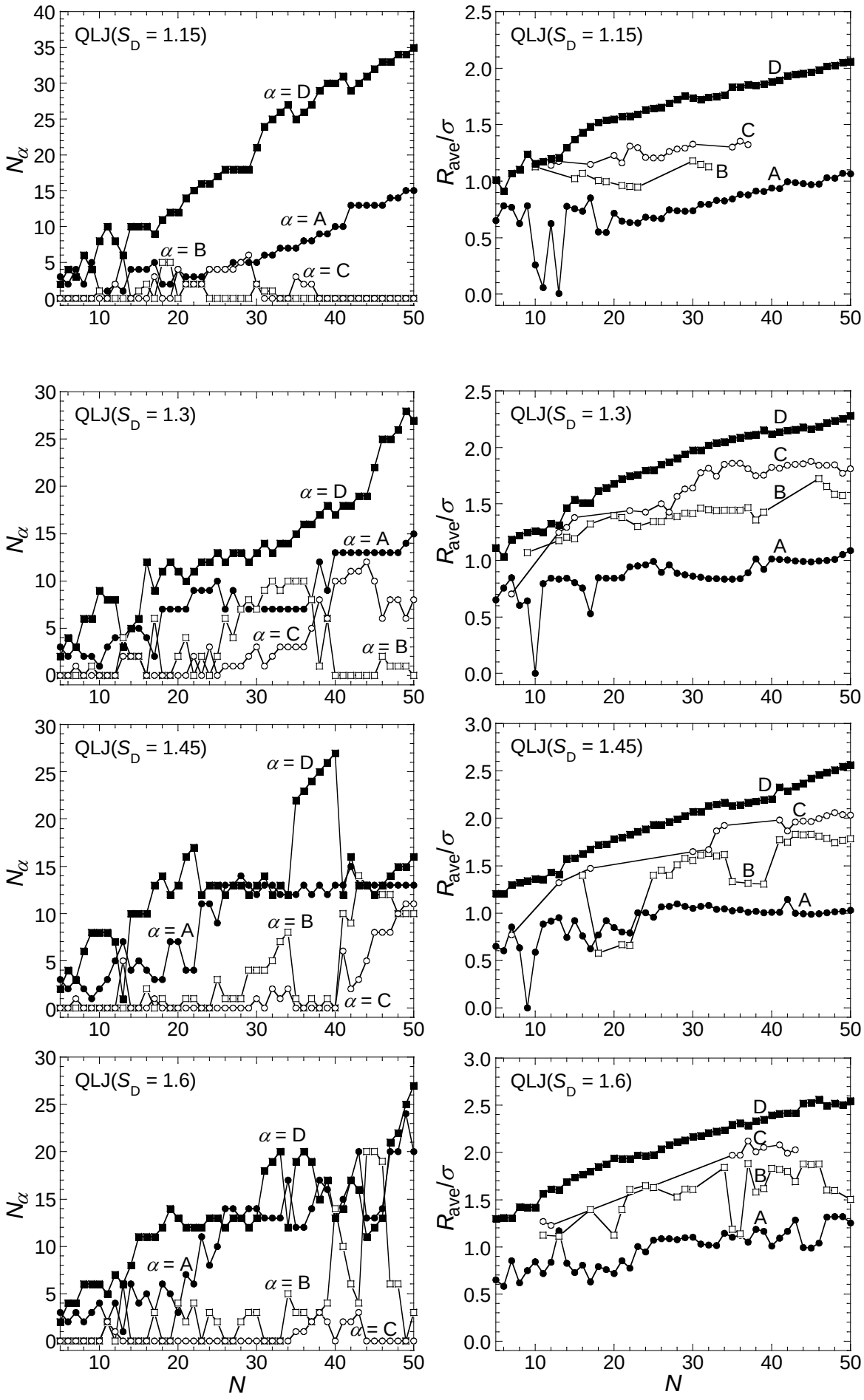
QLJ(S_D = 1.15)
N_α
α = D
α = A
α = B
α = C
R_{ave}/σ
D
C
B
A
QLJ(S_D = 1.3)
QLJ(S_D = 1.45)
QLJ(S_D = 1.6)
N

Figure 3

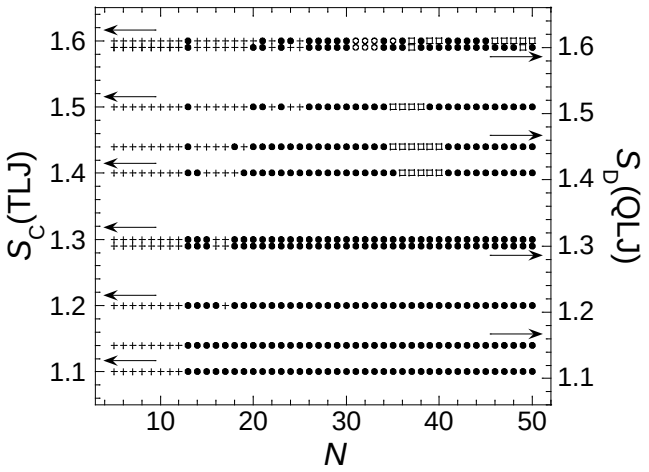

Figure 4

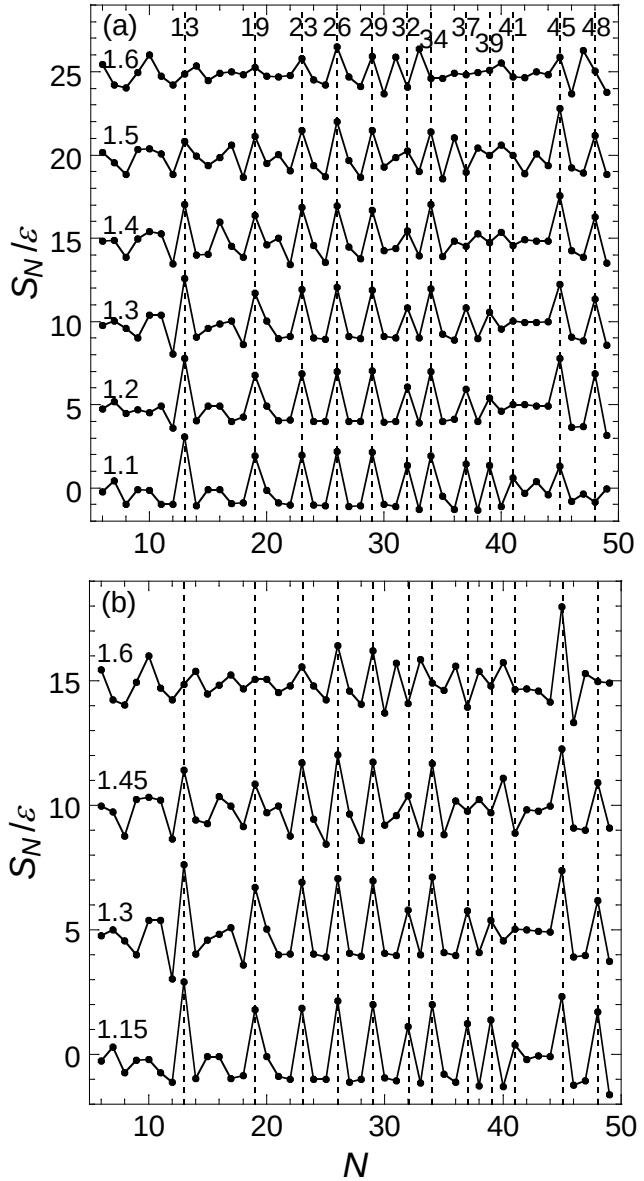

Figure 5

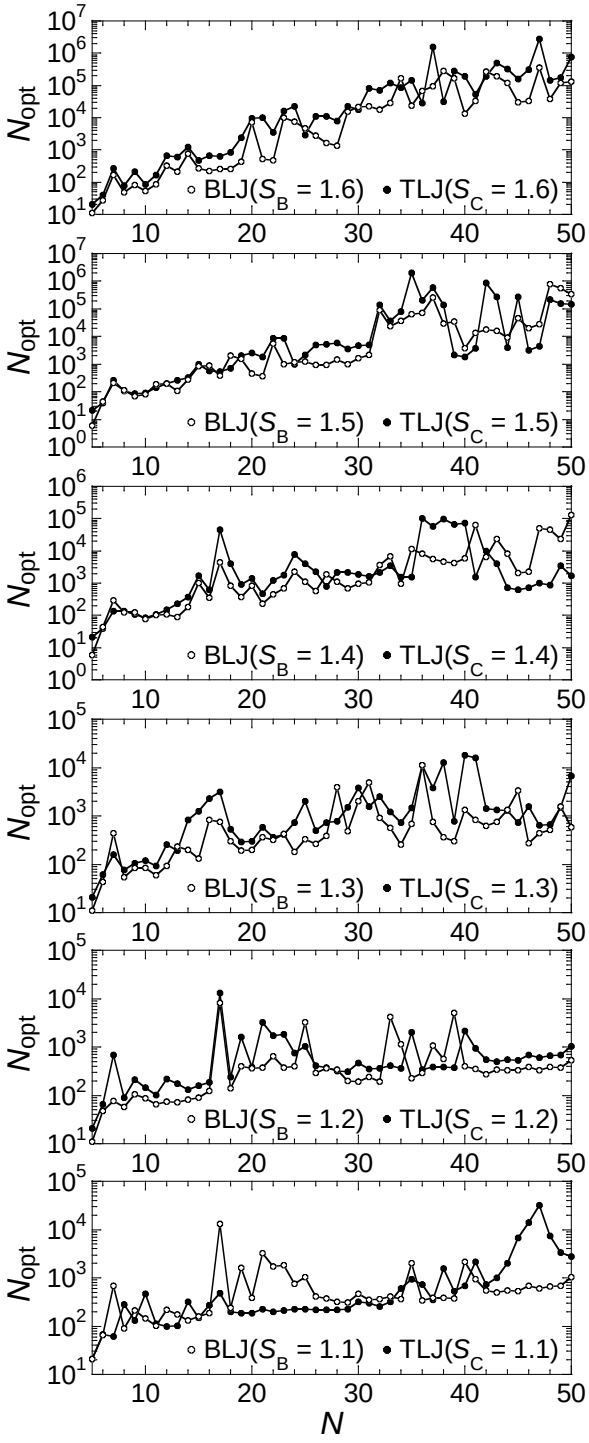
N_{opt}
BLJ(S_B = 1.6) TLJ(S_C = 1.6)
BLJ(S_B = 1.5) TLJ(S_C = 1.5)
BLJ(S_B = 1.4) TLJ(S_C = 1.4)
BLJ(S_B = 1.3) TLJ(S_C = 1.3)
BLJ(S_B = 1.2) TLJ(S_C = 1.2)
BLJ(S_B = 1.1) TLJ(S_C = 1.1)
10 20 30 40 50
N

Figure 6

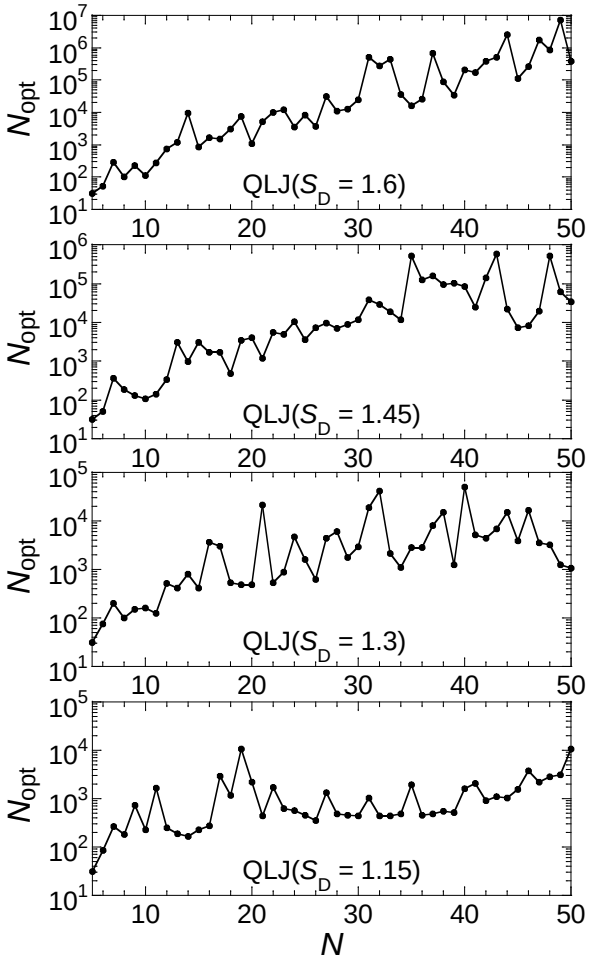

Figure 7

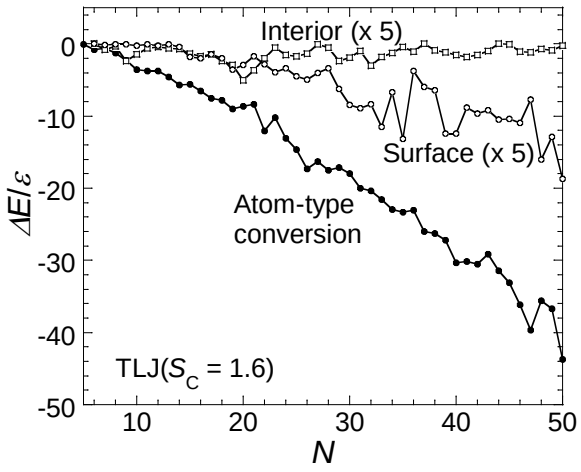
Interior (x 5)
Surface (x 5)
Atom-type
conversion
TLJ(S_C = 1.6)
$\Delta E/\varepsilon$
N
0
-10
-20
-30
-40
-50
10
20
30
40
50

Figure 8